Design Optimization of Building Form and Fenestration for Daylighting and Thermal Energy in Three Variations of the Hot Climate of Egypt

Amany Khalil[1]*
[1]Department of Architectural Engineering, Faculty of Engineering & Technology, Future University in Egypt, 90th St, First New Cairo, Cairo Governorate 11835, Egypt.
*amany.medhat@fue.edu.eg

Abstract

Early consideration of building form and orientation in architectural design can significantly reduce a building's energy consumption, crucial due to the built environment's contribution to climate change crisis. Previous research using optimization of building form for energy performance in more than one city focused mainly on the difference between three or more major climates. However, the difference between cities that are variations of the same climate is not fully studied. This research proposes a multi-objective-optimization (MOO) method of a three-floor office building in three cities that represent variations of the Egyptian climate, Cairo, Alexandria, and Aswan. Dynamic parameters are the building expansion along east-west, floors expansion along north-south, orientation, skylight, WWR, and shadings. Enhancements of one of overall best solutions are 19.63 %, 13.2 %, and 30.1% for annual thermal Energy Use Intensity (EUI), and 8.05%, 11.66%, and 1.54% for annual Useful Daylight Illuminance (UDI (100-2000)) in comparison to the initial form. The results are compared, and characteristics attributed to the specific conditions of each city are identified. Scatterplots are then developed to study the relationship between building dynamic parameters and the performance objectives. Scatterplots of floors' expansion, building expansion and skylight show the most obvious trends in the three cities.

Highlights

- Optimization of building form and envelope.
- Considerations of three variations of the same climate.
- " Ladybug and Honeybee " simulations.
- Multi-objective genetic algorithm "Octopus" to enhance building performance

Introduction

Concerns over supply difficulties, exhaustion of energy resources and heavy environmental impacts has already been raised by the rapid growth in the usage of world energy (Pérez-Lombard et al., 2008). The growth in population, the increase in the time spent inside buildings, increase in the building functions and indoor environmental quality, and climate change led to a great increase in the energy consumed by the built environment (Cao et al., 2016). The increase in the consumption of Egyptian electricity in recent years is expected to grow higher with significant impacts on economic and social aspects (Elharidi et al., 2017). The building sector share

in the consumption of Egyptian electricity is about 66%–74%, and the amount of energy it consumes has unprecedently increased Over the past decade(Emil & Diab, 2021).

The building form is considered among the most important parameters that affect heat loss through the whole building envelope (Oral & Yilmaz, 2002). Optimization for building energy performance in the early stage of the design process helps in saving energy and reducing greenhouse gas emissions in the building sector (Jin & Jeong, 2014). Determining the form of a building is the primary activity in the architecture design process (Song H et al., 2016). However, traditional methods of architectural conceptual design manipulate the building form mainly for visual and functional aspects and postpone energy consideration to later stages to be conducted by specialized engineers, whereas performative architectural form responds mainly to building performance (Turrin et al., 2011). Many office buildings in Egypt adopt the concept of rigid basic forms and do not consider passive techniques applied to building forms to enhance thermal energy and daylighting performance. In addition, they use fully glazed facades with no shading devices specially in new cities, and this does not suit Egypt hot arid climate as it causes the increase in cooling loads in the summer thereby increases the energy consumed by the building (Ahmad & Reffat, 2018; Elkhayat et al., 2020; M. ElBatran & Ismaeel, 2021a). Even though there is a growing need for studies that build a system for optimization of building form, orientation, and envelope to enhance thermal energy and daylighting performance in Egypt. Most of energy performance and daylighting optimization studies, especially those performed on Egyptian buildings, use rigid building form and limit the variables to envelope parameters such as shading devices, walls retrofitting, façade design, and skylight (Abdel-Rahman, 2021; Ayoub, 2019; Chatterjee & Chowdhury, 2017; Emil & Diab, 2021; M. ElBatran & Ismaeel, 2021a, 2021b; Marzouk et al., 2020; Samaan et al., 2018).

In the new millennium, many studies were conducted that use optimization of building form for energy performance emphasizing on the importance of building shape and orientation in saving a considerable percentage of the total energy consumed by a building. Many of these studies considered more than one major climate zone showing how the optimal building form changes in accord with the change in climate conditions. For example, L. Caldas

(2008); L. G. Caldas & Norford (2003) optimized residential building for daylighting and heating energy in three different climates (hot, temperate and cold) in the USA. The residential building consisted of two floors in which each floor was divided into four adjacent rooms. Yi & Malkawi (2012) optimized one zone of a complex building form to enhance energy performance in hot, cold, and temperate cities. Jin & Jeong (2014) optimized top polygon, top length, tilt angle, twisted angle, and azimuth angle of a single zone free form building for thermal performance in 14 different cities with five different climate zones. The form was hypothetical, and the building function was not considered. Caruso & Kämpf (2015) optimized different types of building forms for energy consumption resulted from solar irradiation in Basel and Dubai without mentioning building type. Konis et al. (2016) optimized a three-floor open office building for UDI and EUI incorporating mixed mode natural ventilation in Los Angeles, Helsinki, Mexico City, and New York City while considering real urban contexts. Fang & Cho (2019) manipulated building depth, location of roof ridge, three skylights, south and north windows widths, louver length of a single floor open office building for EUI and UDI in Miami (hot), Atlanta (mixed), and Chicago (cold). Khalil et al. (2021) optimized opaque building form for thermal energy performance in Cairo, London, and Chicago. Lu et al. (2021) optimized WWR, orientation, and aspect ratio of a square shaped office building form, and the Courtyard scale, WWR, positions of points construct the form of a quadrilateral office building form in Beijing (Cold), Shanghai (Humid Subtropical-fully humid), and Shenzhen (Humid Subtropical-dry winter). Khalil et al. (2023) optimized a cellular office building form for thermal energy performance in Cairo (arid), London (temperate) and Chicago (cold).

On the other side, some studies considered just one city. For example, Yi & Malkawi (2009) optimized a single zone building to enhance its energy performance in Philadelphia. Rodrigues et al. (2014) generated 12 alternative floor plans for two sets of houses to enhance their thermal performance in City of Coimbra, Portugal. Chen et al. (2018) optimized a building form in Singapore for daylighting, cooling systems and cooling energy consumption. Taleb et al. (2020) optimized floor number, floor height, number of vertices in floor to reduce incident solar radiation in a Mediterranean city at a latitude of 33.5 degrees. Dong et al. (2021) optimized height and width of an office building located in the north-east of China for EUI, Daylight Autonomy, and UDI. Khalil et al. (2023) optimized form and envelope, of a cellular office building in Cairo, for thermal energy, daylighting and views percentage to the outdoor. Khalil, Lila, et al. (2023) Optimized and predicted the energy performance of multiple proposed form generation methods in Cairo using genetic algorithm and machine learning.

There is still a lack of studies that optimizes building form for energy performance considering different variations of cities within the same major climate. Especially for office building forms with their high percentage of energy consumption in comparison to the built environment. This research proposes a MOO method of building form and envelope at the early stage of the design process for architects who work on Egyptian projects. The MOO method generates diversity of simple and complex building forms and examines their energy and daylighting performance. This MOO framework integrates parametric design of building form and envelope, thermal energy and daylighting simulations, and multi-objective genetic algorithm. The applicability of the proposed method is demonstrated through the usage of a three-floor open plan office building. The optimal produced forms in each of the three cities are discussed and compared together. Finally, scatterplots are developed that show the relationship between dynamic parameters of building form and envelope and performance objective functions.

Research framework

The proposed MOO workflow and the required tools (red font) are presented in Figure1. This workflow includes four main steps, parametric modelling of building thermal zones, modelling the building envelope, adding thermal EUI and UDI simulations, and running MOO. The workflow steps are explained below.
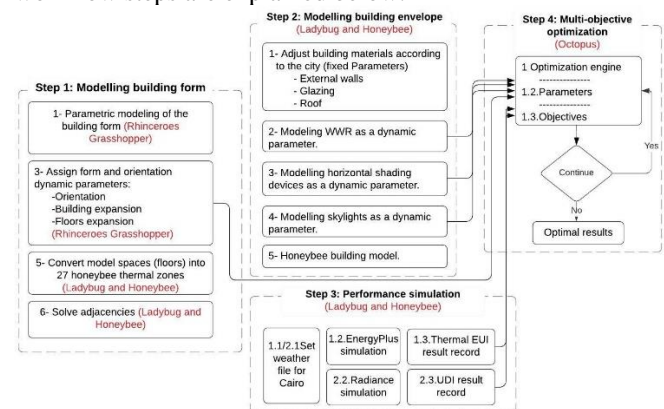

Figure 1: Proposed workflow shows sequential stages.

Modelling building form and envelope

Grasshopper, and rhinoceros 6 (Robert McNeel & Associates, 2021) are used to parametrically model the building form. The initial building is a low-rise open-plan office building with a square shaped plan (Fig.2), WWR 30 %, no skylights, and orientation 0 rad. This initial form is simulated first for each of the three cities to be used as the experiment base case. It is 12 m * 12 m with total height 9m, total built up area 432 m2 and total volume 1296 m3. The building is considered as three thermal zones in the energy simulation. Table 1 shows static parameters fixed across the three cities.

Figure 2: Initial squared building form.

Table 1: Static parameters fixed in the three cities.

Static parameters	value
Floors number (thermal zones)	3
Floor Height	3 m
The height of the whole building	9 m
Number of windows in each floor	4
Windows sill height	0.8 m
Window height from sill	2 m
Window centerline	fixed
Skylight centerline	fixed
Roof shape of each floor	flat

Table 2 shows building dynamic parameters with their initial values and ranges. There are two variables for building form, the expansion of the whole building along east-west axis and the expansion of each floor along north-south axis. The orientation is also considered as a dynamic parameter (anti-clockwise direction). In addition, three envelope parameters are considered as dynamic parameters, skylights, WWR, and horizontal shading devices. For both forms dynamic parameters, the ranges in Grasshopper are normalized to 1 to 2, and they vary by 0.1. These expansion values are percentages (factor) as the initial building value is assumed to be 1 and then it is multiplied bu these values. For building orientation, the range is normalized to 0 to 2, and it vary by 0.1. Its initial value is set to 0. Orientation values are in radians. Sky light initial ratio with the roofs is set to 0, and it has three other values during optimization, 10, 20, and 30 %. Where one skylight could be generated in each roof. WWR initial value is set to 30%, and it has two other values during the experiment, 60% and 90%. Each façade in each floor has one window. Horizontal shading devices with two shades on each window are considered as dynamic parameters for each of the four facades. Shading devices initial value is set to 0, and it has two other values during the experiment, 0.5 and 1. There are dynamic parameters that depends on other dynamic parameters. For example, skylight is formed on the roof of the third floor in the base case. Its quantity increases when two or one floor expand to create new exposed roofs. Its quantity also changes with the change in the building expansion dynamic parameter.

Table 2: Form, orientation and envelope dynamic parameters for the three cities with the north direction.

parameter	Building expansion along east-west	Floors expansion along north-south axis	Building rotation (Rad.)	Skylight (%)	WWR in each facade (%)	Shading devices (m)
No.	1	3	1	1	4	4
values	1,1.1,1.2,1.3,1.4,1.5,1.6,1.7,1.8,1.9, and 2. Values are in percentages.	1,1.1,1.2,1.3,1.4,1.5,1.6,1.7,1.8,1.9, and 2. Values are in percentages.	0, 0.1, 0.2, 0.3, 0.4, 0.5, 0.6, 0.7, 0.8, 0.9, 1, 1.1,1.2,1.3,1.4,1.5,1.6,1.7, 1.8,1.9, and 2.	0, 0.1, 0.2, 0.3.	0.3, 0.6, 0.9.	0, 0.5, 1.

Thermal energy and daylighting

The Köppen climate classification scheme describes climate conditions in reference to multiple variables and their seasonalities using one metric (Figure 3) (D. Chen & Chen, 2013).
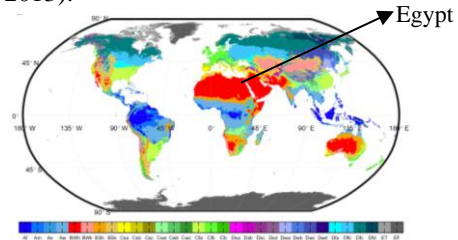

Figure 3: Köppen climate sub-types of the five major groups. (Source: D. Chen & Chen, 2013)

For this study, three variations within the Egyptian hot-arid climate are chosen as case studies namely Cairo, Alexandria, and Aswan. Figure 4A shows the annual temperature range while figure 4B shows the annual sky cover range for each of the three cities. Ladybug and Honeybee (Sadeghipour Roudsari, 2021) are used to add three EnergyPlus EPW weather files, to perform Thermal energy simulation using EnergyPlus, and to perform daylighting simulation using Radiance. Ladybug and Honeybee assign automatically data needed to perform energy and daylighting simulation. Table 3 shows example of these automatically assigned data while table 4 shows data edited by the author for each city in reference to literature (Khalil, Tolba, et al., 2023; Konis et al., 2016) according to its specific climate using the "Honeybee search EnergPlus construction" component (Sadeghipour Roudsari, 2021). Both tables include data that are fixed throughout the experiment.

Since the building area changes during optimization, thermal EUI (annual energy consumed by a unit area of a building) is used to calculate the annual thermal energy consumed per unit area instead of calculating the whole building thermal energy. In order to initiate UDI-(100-2000) simulation, daylighting sensors dots are placed with a test grid size 4m and 0.7m distance above each floor.

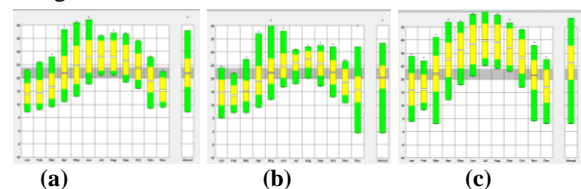| (a)	(b)	(c)

Figure 4A: Annual temperature range for each city, a: Cairo, b: Alexandria, c: Aswan (source: (Climate Consultant. Get the Software Safely and Easily., 2023).
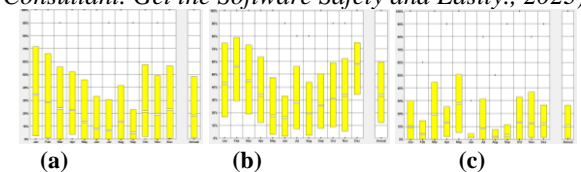

(a)	(b)	(c)

Figure 4B: Annual sky cover range for each city, a: Cairo, b: Alexandria, c: Aswan (source: (Climate Consultant. Get the Software Safely and Easily., 2023).

BS 2023
4-6 SEPT
SHANGHAI

International
Building
Performance
Simulation
Association

Table 3: Static parameters assigned automatically by ladybug and honeybee in the three cities.

Static parameters	Values
Interior & exposed floors U-value	1.449209 W/m2-K
Interior walls U-value	2.58 W/m2-K
Illuminance threshold for daylight autonomy	300 lux
Lighting density per area	11.84 W/m2
Equipment load per area	7.64 W/m2
Lighting control type	Auto dimming with switch off occupancy sensor
Infiltration rate per area	0.0002 m3/s m2
Number of people per area	0.0565 ppl/m2
Ventilation per area	0.0003 m3/s m2
Ventilation per person	0.0024 m3/s

Table 4: Building parameters fixed within each location.

Static parameters	Cairo-climate zone 2B	Alexandria-climate zone 2A	Aswan-climate zone 1B
Ext.walls	CBECS 1980-2004 Ext. Wall MASS, Climate Zone 2B	CBECS 1980-2004 Ext. Wall MASS, Climate Zone 2A	CBECS 1980-2004 Ext. Wall MASS, Climate Zone 1
Ext. walls U-value	3.573262 W/m2-K	2.715218 W/m2-K	3.690821 W/m2-K
Window	ASHRAE 189.1-2009 Ext. Window climate zone 2B	ASHRAE 189.1-2009 Ext. Window climate zone 2	ASHRAE 189.1-2009 Ext. Window climate zone 1
Glazing U-value	13.833333 W/m2-K	13.833333 W/m2-K	702.433333 W/m2-K
Roof	CBECS 1980-2004 EXTROOF IEAD CLIMATEZONE 2B	CBECS 1980-2004 EXTROOF IEAD CLIMATEZONE 2A	CBECS 1980-2004 EXTROOF IEAD CLIMATEZONE 1 & 5B 1
Roof U-value	0.274975 W/m2-K	0.403797 W/m2-K	0.457037 W/m2-K 0.301575 W/m2-K

Optimization and scatterplots

Octopus (based on SPEA-2 and HypE algorithm) is a genetic algorithm plug-in for Rhino-grasshopper that presents the approach of Pareto front for multi-objective optimization (Vierlinger, R., 2021). The concept of a Pareto- optimal is that it provides a set of best alternatives that are non-dominated solutions (Machairas et al., 2014). Octopus is used in this study to perform optimization with the objectives of minimizing annual thermal EUI and maximizing annual UDI (100-2000) while imposing genetic diversity as a third objective. Octopus works on minimizing objectives functions only. Therefore, UDI (100-2000) results' values are multiplied by -1 during optimization. After finishing each experiment, the enhancement percentages of each of the two objectives in the selected optimal results are calculated in comparison to the base case. Before starting the optimization, generations number is adjusted to six (from zero to five) in the Octopus user interface. TT toolbox is used to record the values of dynamic parameters and their corresponding objectives' values to develop scatterplots. Scatterplots shows the relationship between chosen building form and envelope dynamic parameters and the enhancement percentage of objective functions in comparison to the base-case.

Results and discussion

The results demonstrate the applicability of the proposed method in enhancing thermal EUI and UDI of an open office building in three variations of the arid climate of Egypt. In comparison to the base case, Cairo EUI was enhanced by 35.1% and UDI by 9.49. One of the overall best solutions (tradeoff) enhanced EUI by 19.63% and UDI by 8.05%. Alexandria EUI by 36.14 and UDI by 15.15. One of the overall best solutions enhanced EUI by 13.2 % and UDI by 11.66 %. Aswan EUI by 10.74 and UDI by 5.99%. One of the overall best solutions enhanced EUI by 30.1% and UDI by 1.54%. Figure 5 shows optimization results' Pareto graphs for Cairo, Alexandria, and Aswan after optimization. Each cube in a graph represents an iteration. Each graph includes all the simulated iterations with the Pareto front ones highlighted with yellow. The top row shows the relationship between EUI and UDI, while the bottom row shows the 3-D pareto front including genetic diversity. The iterations in the corner of the pareto- front are the non-dominated solutions where two overall best solutions are selected from them.
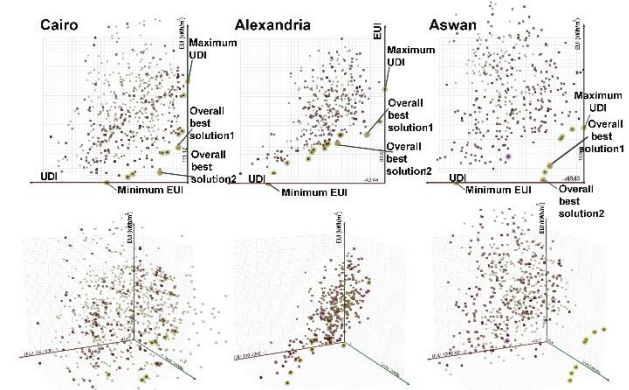

Figure 5: Optimization results' graphs for the three cities with pareto front solutions highlighted.

For each city UDI, thermal EUI optimal solutions and two overall best solutions (non-dominated) are presented in Figures 6,7 and 8. Table 5 shows values of dynamic parameters for each solution. The value of EUI, in addition to the improvement percentages of EUI and UDI in comparison to the base case are presented for each of the four optimal solutions (a: Total thermal EUI (kWh/m2), b: Thermal EUI improvement percentage, c: UDI-(100-2000) improvement percentage). Positive percentages indicate better performance while negative percentages indicate lower performance in comparison to the base case. The following discussion compares the results of the three cases and identifies characteristics attributed to the specific conditions of each city. Despite that the three cities fall in the major hot-arid climate of Egypt, they still have some variations as shown above (figure 4A &4B) that resulted different optimal results as discussed below. The main focus is on the general

characteristics of the 12 design configurations that is summarized below:

1. Optimal solutions in terms of UDI have similar skylight to roof ratio in both Alexandria and Aswan (10%) and a higher ratio in Cairo case (20%). All EUI best solutions and the chosen overall best solutions do not have skylights except for the first overall best solution in Alexandria.

2. Even though the building expansion seems to be effective in each of the 12 designs, the percentages vary from one case to another, and the highest expansion is in Aswan Case (1.9 % for all cases).

3. Generally, the expansion of floors seems to be beneficial for all designs with variations in percentages. The highest expansion percentages are in the first (ground) floor in all of the 12 design solutions.

4. All Thermal EUI best solutions, in addition to the overall best solutions in the three cities have shading devices in all facades with different protrusion length. Only EUI optimal solution in Alexandria reaches the maximum shading length in all facades. All UDI best solutions have shading devices in all facades except for north-west and north-east facades of Cairo's UDI best solution and north-east façade of Alexandria's UDI best solution that have no shading devices.

5. Many of WWR values are increased in all of the 12 designs with different values. The maximum value is reached in the north-east façade of one of Cairo's overall best solutions, the north-west, south-east, and north-east facades of Alexandia's UDI best solution. In addition to the south-west façade of second overall best solution in Alexandria and the north-west facades of Aswan's best EUI and first overall best solutions.

		Max. UDI	Min. EUI	Best 1	Best 2
		0.3-0.6	0.6-0.3	0.3-0.9	0.3-0.3
	Shading devices (m) N-W-S-E	0-1-1-0	1-1-1-0.5	1-1-1-0.5	1-1-1-0.5
Alexandria	Building exp.(%)	1.3	1.7	1.5	1.8
	Floors Exp.(%)1st 2nd- 3rd	1.9-1-1.2	1.9-1.5-1.6	1.5-1-1.1	1.8-1-1.2
	Rotation (rad.)	0.1	1.9	0.3	0.4
	Skylight(%)	0.1	0	0.1	0
	WWR – N-W-S-E	0.9-0.6-0.9-0.9	0.3-0.3-0.6-0.3	0.6-0.3-0.6-0.6	0.6-0.9-0.6-0.3
	Shading devices (m) N-W-S-E	0.5-1-1-0	1-1-1-1	1-1-1-0.5	0.5-0.5-0.5-0.5
Aswan	Building exp.(%)	1.9	1.9	1.9	1.9
	Floors Exp.(%)1st 2nd- 3rd	2-1-1.3	1.9-1.3-1.8	1.8-1.1-1.1	1.9-1.1-1.1
	Rotation (rad.)	0.4	1.8	0.2	0.4
	Skylight(%)	0.1	0	0	0
	WWR – N-W-S-E	0.6-0.6-0.6-0.6	0.9-0.6-0.3-0.6	0.9-0.6-0.6-0.6	0.6-0.6-0.6-0.3
	Shading devices (m) N-W-S-E	0.5-1-0.5-0.5	1-1-0.5-1	0.5-1-1-0.5	0.5-1-1-1

Figure 6 content (columns: Building physical design perspective | Building physical design layout | Thermal EUI for each zone | UDI (100-2000) in each floor):
- Max. UDI — a:187.87, b: -9.7%, c:9.49%
- Min. EUI — a:111.12, b:35.1%, c:-2.99%
- Best 1 — a:137.63, b:19.63%, c:8.05%
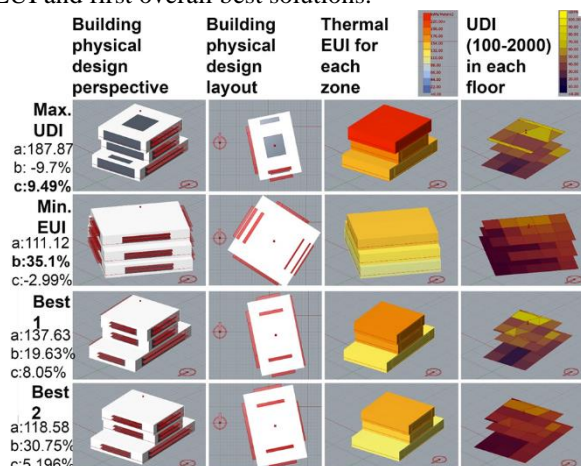- Best 2 — a:118.58, b:30.75%, c:5.196%

Figure 6: Optimal solutions for Cairo.

Table 5: parameter's values for each solution.

	Dynamic parameter	Max. UDI	Min. EUI	Best 1	Best 2
Cairo	Building exp.(%)	1.1	1.7	1.1	1.3
	Floors Exp.(%)1st 2nd- 3rd	1.6-1-1.2	1.8-1.6-1.2	1.9-1-1.1	1.9-1-1.1
	Rotation (rad.)	0.2	1	0.2	0.2
	Skylight(%)	0.2	0	0	0
	WWR – N-W-S-E	0.6-0.6	0.3-0.3	0.3-0.6	0.3-0.6

Figure 7 content (columns: Building physical design perspective | Building physical design layout | Thermal EUI for each zone | UDI (100-2000) in each floor):
- Max. UDI — a:141.54, b:-8.11%, c:15.15%
- Min. EUI — a:83.6, b:36.14%, c:-17.01%
- Best 1 — a:113.64, b:13.2%, c:11.66%
- Best 2 — a:108.2, b:17.4%, c:5.2 %
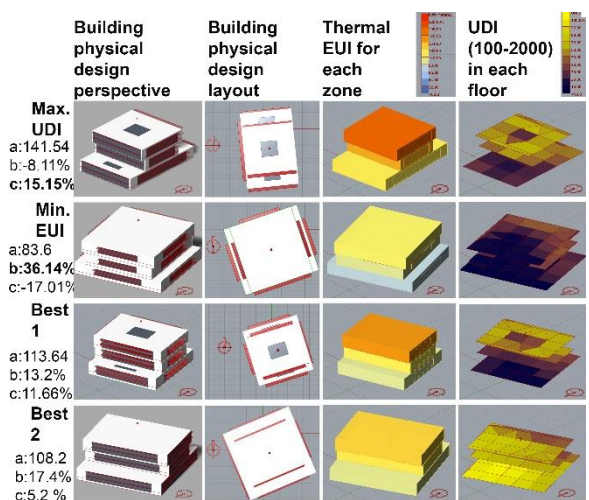
Figure 7: Optimal solution for Alexandria.

Figure 8 content (columns: Building physical design perspective | Building physical design layout | Thermal EUI for each zone | UDI (100-2000) in each floor):
- Max. UDI — a:221.02, b:16.64%, c:5.99%
- Min. EUI — a:169.7, b:35.99%, c:-10.74%
- Best 1 — a:185.49, b:30.1%, c:1.54%
- Best 2 — a:172.25, b:35.03%, c:0.64%

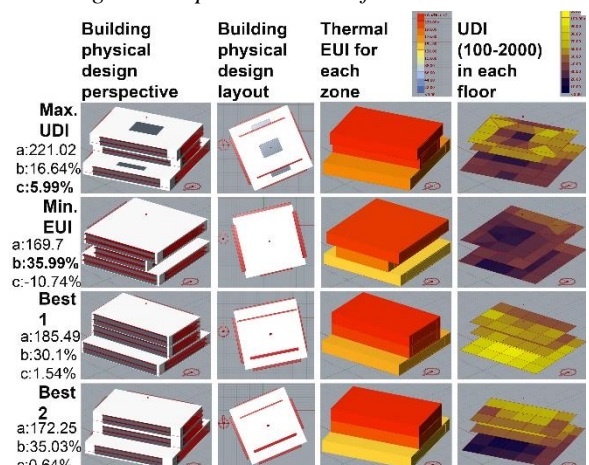*Figure 8: Optimal solution for Aswan.*

Scatterplots

After performing the optimization, scatterplots are developed using data of all simulated iterations in each of the three experiments. Each scatterplot shows the relationship between one dynamic parameter and the improvement percentage of one objective function. Points

BS 2023
4 - 6 SEPT
SHANGHAI

International
Building
Performance
Simulation
Association

in a scatterplot represent all iterations in the experiment. Trend line is presented in each scatterplot to show whether it has a positive or negative impact on the enhancement of each objective function in reference to the base case. Scatterplots that show the highest obvious trend are building expansion, average expansion of floors, and skylight percentage presented in Figures 9 and 10.

Both building expansion and average expansion of floors proved to have high positive impact on thermal EUI and negative impact on UDI (100-2000) in the three cities. However, impacts of average expansion of floors differ from city to city. While average expansion of floors shows an obvious positive trend in enhancing thermal EUI in Cairo (R^2= 0.153), it shows a slight positive trend in Alexandria and a very low positive trend in Aswan (R^2= 0.0056). On the other side, it has a higher negative impact on UDI (R^2= 0.2055) in Cairo than in Alexandria and then Aswan (R^2= 0.0369). Scatterplots of skylight shows it has negative impact on enhancing thermal EUI in the three cities with almost similar decreasing trend. On the other side, skylight proved to enhance UDI in both Cairo and Alexandria with the same increasing trend. But it has slight negative impact on UDI on Aswan.
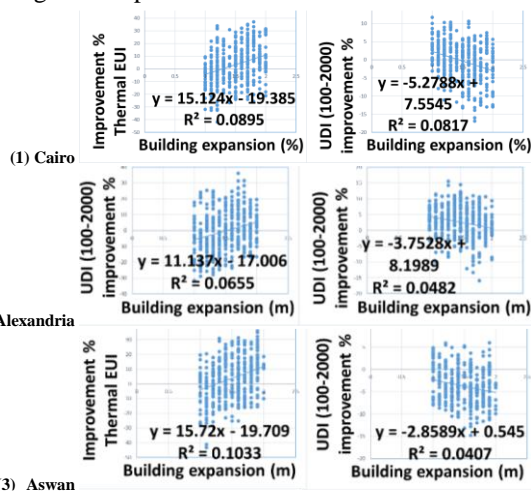

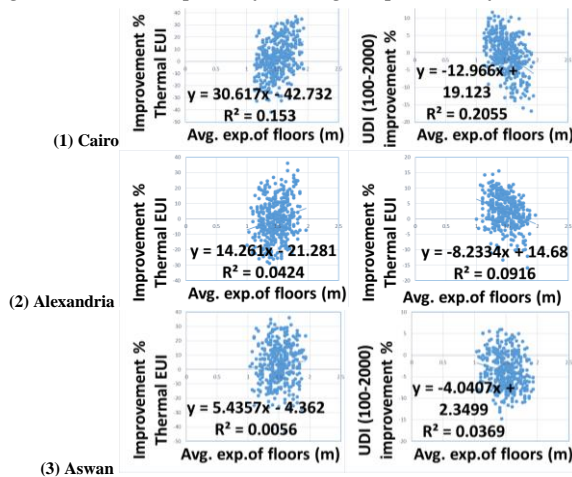*Figure 9A: Scatterplots of average expansion of building*

Figure 9B: Scatterplots of average expansion of floors.

The trend in scatterplots of other dynamic parameters is not as strong as the trend shown in scatterplots of the form

and skylight parameters. The figures of these other dynamic parameters show scatterplots with R^2 greater than or equal to 0.01 0nly. Scatterplots of orientation (Figure 11) shows it has a slight increasing trend towards enhancing thermal EUI in each of the three cities with a stronger effect in Aswan R^2= (0.0144) and lower in both Cairo (R^2= 0.006) and Alexandria (R^2=0.008). There is no trend towards enhancing UDI in Cairo (R^2 = 7E-05) and a very slight decreasing trend in Alexandria (R^2 = 0.0044) and a clearer decreasing trend in Aswan (R^2 = 0.0194). Scatterplots in Figure12 show that increasing WWR value in all facades has a decreasing trend towards enhancing thermal EUI in each of the three cities except for north façade in Aswan that has a positive increasing trend. This decreasing trend varies from city to city. For example, the east façade in Cairo shows a slight decreasing trend towards enhancing EUI, but the east façade in Alexandria shows an obvious decreasing trend. On the other side, increasing WWR in all facades shows an increasing trend towards enhancing UDI in the three cities with slight differences in the trend. However, this does not apply to the manipulation of WWR in North facades in both Cairo and Alexandria that shows almost no trend.

Scatterplots presented in Figure 13 show that the manipulation of shading devices in all facades has a positive impact towards enhancing thermal EUI in the three cities with a slight variation in the increasing trend. This does not apply to shading devices in the east façade in Cairo and shading devices in the north façade in Aswan that show almost no trend. Where protrusion of the shading devices in the east and south façades in Cairo show an increasing trend towards enhancing UDI, they show a slight decreasing trend in the north façade and almost no trend in the west façade. Shading devices in Alexandria show a slight decreasing trend towards enhancing UDI in all facades except for west façade that shows almost no trend. In Aswan, shading devices show an increasing trend towards enhancing UDI in all facades except for the east façade that shows almost no trend.
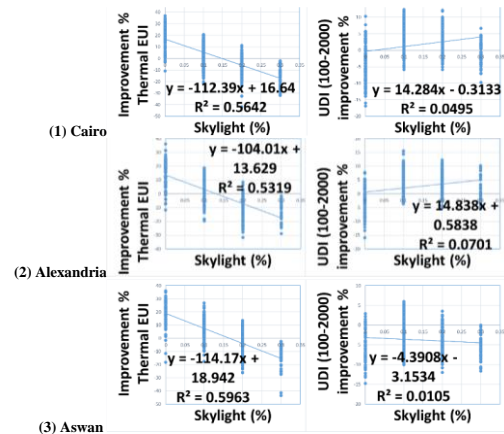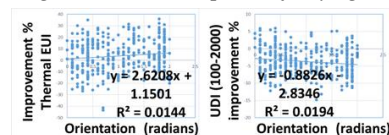

Figure 10: Scatterplots of skylight.
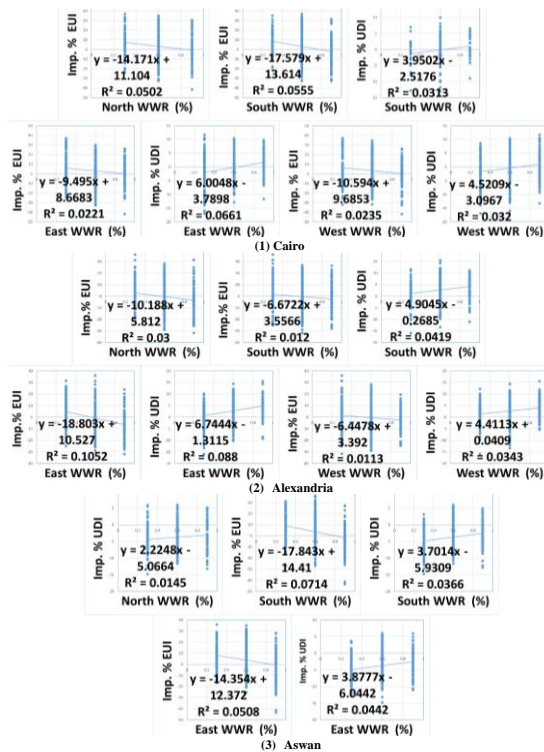

Figure 11: Scatterplots of orientation values (radians).

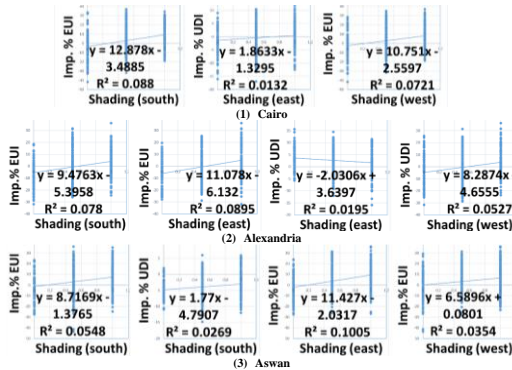*Figure 12: Scatterplots of WWR (%) in each façade.*

Figure 13: Scatterplots of shading devices (m).

Conclusion

This study proposes a MOO method to enhance office building performance at the early design stage in three variations of the hot arid climate of Egypt. This MOO method uses parametric design, thermal energy simulation, daylighting simulation, and multi-objective genetic algorithm. It generates alternative design configurations, tests their thermal energy and daylighting performance while considering genetic diversity, and find best solution for each objective in addition to overall best solutions. Form and envelope parameters are optimized for a three-floor building that represents an open plan office building. The three cities are Cairo, Alexandria, and Aswan, and the manipulated design parameters are the building form, orientation, skylights ratio, WWR, and shading devices. After performing the optimization, best solutions for each of the two objectives are identified, in addition to two of overall best solutions. Enhancements of one of overall best solutions are 19.63 %, 13.2 %, and 30.1% for annual thermal EUI, and 8.05%, 11.66%, and 1.54% for annual UDI (100-2000) in comparison to the initial

squared form. The annual thermal EUI is decreased by 30.75%, 17.4%, 35.03%, and annual UDI (100-2000) is increased by 34.93%, 5.2%, and 0.64% in comparison to the initial squared form. The results of the three variations of the hot arid climate are then compared and characteristics attributed to specific climate conditions of each city are identified. Finally, scatterplots are developed to show the relationship between dynamic parameters and objective functions. Scatterplots that show the most obvious trend are expansion of floors, expansion of building and skylight ratio.

Future applications to variations in other climate zones are recommended to expand the current work. The inclusion of more objectives such as, natural ventilation, cost, structure, etc. is also recommended. Since roof shape affects energy and daylighting objectives, future work is needed also to include the manipulation of the roof shape while keeping the volume constant. Also, the inclusion of more dynamic parameters and the examination of their relationship with objectives is needed. Future work is needed also to apply the same method to different types of buildings in Egypt such as residential, healthcare, educational, etc.

Acknowledgements

References

Abdel-Rahman, W. S. M. (2021). Thermal performance optimization of parametric building envelope based on bio-mimetic inspiration. *Ain Shams Engineering Journal*, *12*(1), 1133–1142.

Ahmad, R. M., & Reffat, R. M. (2018). A comparative study of various daylighting systems in office buildings for improving energy efficiency in Egypt. *Journal of Building Engineering*, *18*, 360–376.

Ayoub, M. (2019). A multivariate regression to predict daylighting and energy consumption of residential buildings within hybrid settlements in hot-desert climates. *Indoor and Built Environment*, *28*(6), 848–866.

Caldas, L. (2008). Generation of energy-efficient architecture solutions applying GENE_ARCH: An evolution-based generative design system. *Advanced Engineering Informatics*, *22*(1), 59–70.

Caldas, L. G., & Norford, L. K. (2003). Shape Generation Using Pareto Genetic Algorithms: Integrating Conflicting Design Objectives in Low-Energy Architecture. *International Journal of Architectural Computing*, *1*(4), 503–515.

Cao, X., Dai, X., & Liu, J. (2016). Building energy-consumption status worldwide and the state-of-the-art technologies for zero-energy buildings during the past decade. *Energy and Buildings*, *128*, 198–213.

Caruso, G., & Kämpf, J. H. (2015). Building shape optimisation to reduce air-conditioning needs using constrained evolutionary algorithms. *Solar Energy*, *118*, 186–196.

Chatterjee, T., & Chowdhury, R. (2017). Adaptive Bilevel Approximation Technique for Multiobjective Evolutionary Optimization. *Journal of Computing in Civil Engineering*, 31(3), 04016071.

Chen, D., & Chen, H. W. (2013). Using the Köppen classification to quantify climate variation and change: An example for 1901–2010. *Environmental Development*, 6, 69–79.

Chen, K. W., Janssen, P., & Schlueter, A. (2018). Multi-objective optimisation of building form, envelope and cooling system for improved building energy performance. *Automation in Construction*, 94, 449–457.

Climate Consultant. Get the software safely and easily. (2023, March 18). Software Informer. https://climate-consultant.informer.com/6.0/

Dong, Y., Sun, C., Han, Y., & Liu, Q. (2021). Intelligent optimization: A novel framework to automatize multi-objective optimization of building daylighting and energy performances. *Journal of Building Engineering*, 43, 102804.

Elharidi, A. M., Tuohy, P. G., Teamah, M. A., & Hanafy, A. A. (2017). Energy and indoor environmental performance of typical Egyptian offices: Survey, baseline model and uncertainties. *Energy and Buildings*, 135, 367–384.

Elkhayat, Y. O., Ibrahim, M. G., Tokimatsu, K., & Ali, A. A. M. (2020). Multi-criteria selection of high-performance glazing systems: A case study of an office building in New Cairo, Egypt. *Journal of Building Engineering*, 32, 101466.

Emil, F., & Diab, A. (2021). Energy rationalization for an educational building in Egypt: Towards a zero energy building. *Journal of Building Engineering*, 44, 103247.

Fang, Y., & Cho, S. (2019). Design optimization of building geometry and fenestration for daylighting and energy performance. *Solar Energy*, 191, 7–18.

Jin, J.-T., & Jeong, J.-W. (2014). Optimization of a free-form building shape to minimize external thermal load using genetic algorithm. *Energy and Buildings*, 85, 473–482.

Khalil, A., Lila, A. M. H., & Ashraf, N. (2023). Optimization and Prediction of Different Building Forms for Thermal Energy Performance in the Hot Climate of Cairo Using Genetic Algorithm and Machine Learning. *Computation*, 11(10), Article 10.

Khalil, A., Tolba, O., & Ezzeldin, S. (2021). Design Optimization of Open Office Building Form for Thermal Energy Performance using Genetic Algorithm. *Adv. sci. technol. eng. syst. j. Advances in Science, Technology and Engineering Systems Journal*, 6(2), 254–261.

Khalil, A., Tolba, O., & Ezzeldin, S. (2023). Optimization of an office building form using a lattice incubate boxes method. *Advanced Engineering Informatics*, 55, 101847.

Konis, K., Gamas, A., & Kensek, K. (2016). Passive performance and building form: An optimization framework for early-stage design support. *Solar Energy*, 125, 161–179.

Lu, S., Wang, C., Fan, Y., & Lin, B. (2021). Robustness of building energy optimization with uncertainties using deterministic and stochastic methods: Analysis of two forms. *Building and Environment*, 108185.

M. ElBatran, R., & Ismaeel, W. S. E. (2021). Applying a parametric design approach for optimizing daylighting and visual comfort in office buildings. *Ain Shams Engineering Journal*, 12(3), 3275–3284.

Marzouk, M., ElSharkawy, M., & Eissa, A. (2020). Optimizing thermal and visual efficiency using parametric configuration of skylights in heritage buildings. *Journal of Building Engineering*, 31, 101385.

Oral, G. K., & Yilmaz, Z. (2002). The limit U values for building envelope related to building form in temperate and cold climatic zones. *Building and Environment*, 37(11), 1173–1180.

Robert McNeel & Associates. (2021). *Rhino 6 for Windows and Mac*. https://www.rhino3d.com/

Rodrigues, E., Gaspar, A. R., & Gomes, Á. (2014). Automated approach for design generation and thermal assessment of alternative floor plans. *Energy and Buildings*, 81, 170–181.

Sadeghipour Roudsari, M. (2021). *Ladybug Tools | Home Page*. https://www.ladybug.tools/

Samaan, M. M., Farag, O., & Khalil, M. (2018). Using simulation tools for optimizing cooling loads and daylighting levels in Egyptian campus buildings. *HBRC Journal*, 14(1), 79–92.

Song H, Ghaboussi J, & Kwon T.-H. (2016). Architectural design of apartment buildings using the Implicit Redundant Representation Genetic Algorithm. *Autom Constr Automation in Construction*, 72, 166–173.

Taleb, S., Yeretzian, A., Jabr, R. A., & Hajj, H. (2020). Optimization of building form to reduce incident solar radiation. *Journal of Building Engineering*, 28, 101025. https://doi.org/10.1016/j.jobe.2019.101025

Turrin, M., von Buelow, P., & Stouffs, R. (2011). Design explorations of performance driven geometry in architectural design using parametric modeling and genetic algorithms. *Advanced Engineering Informatics*, 25(4), 656–675.

Vierlinger, R. (2021). *Octopus | Food4Rhino*. https://www.food4rhino.com/app/octopus

Yi, Y. K., & Malkawi, A. M. (2009). Optimizing building form for energy performance based on hierarchical geometry relation. *Automation in Construction*, 18(6), 825–833.

Yi, Y. K., & Malkawi, Ali. M. (2012). Site-specific optimal energy form generation based on hierarchical geometry relation. *Automation in Construction*, 26, 77–91.